

V3D: Video Diffusion Models are Effective 3D Generators

Zilong Chen^{1,2}, Yikai Wang^{1†}, Feng Wang¹, Zhengyi Wang^{1,2}, and Huaping Liu^{1†}

¹ Tsinghua University
chenz122@mails.tsinghua.edu.cn
² ShengShu



Fig. 1: Delicate 3D assets generated by V3D. Our approach can generate high-fidelity 3D objects within 3 minutes.

Abstract. Automatic 3D generation has recently attracted widespread attention. Recent methods have greatly accelerated the generation speed, but usually produce less-detailed objects due to limited model capacity

[†]Corresponding Authors.

or 3D data. Motivated by recent advancements in video diffusion models, we introduce V3D, which leverages the world simulation capacity of pre-trained video diffusion models to facilitate 3D generation. To fully unleash the potential of video diffusion to perceive the 3D world, we further introduce geometrical consistency prior and extend the video diffusion model to a multi-view consistent 3D generator. Benefiting from this, the state-of-the-art video diffusion model could be fine-tuned to generate 360° orbit frames surrounding an object given a single image. With our tailored reconstruction pipelines, we can generate high-quality meshes or 3D Gaussians within 3 minutes. Furthermore, our method can be extended to scene-level novel view synthesis, achieving precise control over the camera path with sparse input views. Extensive experiments demonstrate the superior performance of the proposed approach, especially in terms of generation quality and multi-view consistency. Our code is available at <https://github.com/heheyas/V3D>.

Keywords: Video Diffusion Models · Single Image to 3D · Novel View Synthesis

1 Introduction

With the advancement of diffusion-based image generation, automatic 3D generation has also made remarkable progress recently. Approaches based on Score Distillation Sampling [67] have achieved tremendous success in the field of 3D generation by extracting priors directly from text-to-image diffusion models [14, 18, 44, 58, 99]. However, such optimization-based methods are relatively slow and suffer from mode collapse [93, 99] and the Janus problem [1, 78].

Subsequent efforts have proposed various alternative pathways to address these issues, mainly including directly mapping images into 3D representations [30, 32, 40, 63, 85, 117] (such as Triplane NeRF [8] or 3DGS [35]), or first generating consistent multi-view images then conducting 3D reconstruction to obtain the underlying 3D model [48, 50, 52]. With the increase in 3D data size and model capacity, these methods have reduced the generation time from hours to minutes. However, the training process of these models still exhibits certain limitations; Methods that directly map to 3D representations require training on 3D datasets, making it impractical to leverage higher-quality image data and large-scale pre-trained image diffusion models. Meanwhile, approaches based on multi-view generation face difficulties in directly generating a sufficient number of images for reconstruction due to the requirement of memory-consuming cross-attention or intermediate 3D structure to ensure consistency across views.

Recently, video diffusion models have attracted significant attention due to their remarkable ability to generate intricate scenes and complex dynamics with great spatio-temporal consistency [2, 4, 5, 7, 13, 24, 25, 109]. Many videos incorporate changes in perspectives which provide natural observations of 3D objects from different views [43], enabling the diffusion models to perceive the physical 3D world [7]. Current multi-view generation methods are based on image diffusion models, which can only generate a few views (less than 6). In contrast,

video diffusion models can generate hundreds of frames, which is adequate for downstream 3D tasks. These advancements give us the possibility to generate consistent multi-view images using video diffusion models and then reconstruct underlying 3D assets to achieve high-quality 3D generation. However, reconstruction from multi-views imposes significant demands on consistency which is difficult for current video diffusion models. In this paper, we aim to fully unleash the potential of video diffusion models to perceive the 3D world and inject the geometrical consistency prior to make the diffusion model an effective multi-view generator. In light of this, we propose V3D, a novel approach for 3D generation with video diffusion models. Specifically, we propose to fine-tune video diffusion models on 3D datasets with additional conditions to generate novel views in both object-centric and scene-level scenarios. For object-centric 3D generation, we fine-tune the base video diffusion model on 360° orbit videos of synthetic 3D objects with the front view as a condition. We find that our fine-tuned model can generate reliable multi-views for 3D reconstruction. However, there still exists inconsistency in some details which may diminish the reconstruction quality. To address this, we adopt perceptual loss instead of pixel-wise loss as the reconstruction objective. We employ Gaussian Splatting as the 3D representation due to its reconstruction and rendering efficiency. To further accelerate the reconstruction, we propose a space-carving initialization method for Gaussians, which involves unprojecting multi-view object masks back to 3D space to roughly position the Gaussians on the object’s surface, eliminating the invalid optimizations on empty spaces. Considering the demands of real-world applications, we also propose a novel mesh extraction method that initially extracts the surface using SDF and subsequently refines the appearance on generated views with image-level loss. Furthermore, we demonstrate the effectiveness of our approach in scene-level 3D generation. To achieve precise camera path control and accommodate multi-view input, we integrate a PixelNeRF encoder to enhance the video diffusion model with robust 3D signals. Combined with auxiliary loss and fine-tuning on real-world posed videos, we extend the video diffusion model to generate novel views on an arbitrary camera path given sparse view input. Our contributions are:

- We propose V3D, a framework that first employs a video diffusion model to generate consistent multi-view frames, then reconstructs the underlying 3D content. By fine-tuning on 3D datasets, we successfully boost the ability of geometrical consistency of video diffusion models. Our framework is generally applicable to both object and scene generation.
- We design a reconstruction pipeline tailored for video diffusion outputs to generate high-quality 3D Gaussians or textured meshes. With our designed efficient initialization and refinement, V3D can reconstruct delicate 3D assets within 3 minutes.
- We conduct experiments to validate the effectiveness of V3D. Both object-centric and scene-level experiments show that our method achieves state-of-the-art performance in reconstruction quality and multi-view consistency.

2 Related Work

2.1 3D Generation

Early efforts in 3D generation focus on per-scene optimization methods based on CLIP [17, 31, 36, 59, 70, 73, 92]. DreamFusion [67], the pioneer work, leverages stronger diffusion prior by introducing Score Distillation Sampling that minimizes the difference between rendered images from the underlying 3D assets and the diffusion prior. Subsequent methods have further achieved substantial improvements of this paradigm in quality [14, 44, 99, 114], optimization speed [58, 86], alleviating the Janus problem [1, 18, 42, 78, 80], and have expanded their applications to generative tasks such as editing [16, 29, 65, 98, 116], texture generation [14, 58, 108], and single image-to-3D [69, 82, 87, 95]. Despite great success has been achieved, optimization-based methods still suffer from slow generation speed and low success rates. To overcome these challenges, researchers have explored some non-optimization paradigms. One stream involves first generating consistent multi-view images, and then utilizing reconstruction methods to obtain the corresponding 3D model [47, 48, 88, 89]. SyncDreamer [50] combines explicit voxels and 3D convolution with a diffusion model to enhance the consistency of generated multi-views. Wonder3D [52] fine-tunes image diffusion models to generate sparse views with corresponding normal maps and utilizes a NeuS [94] to reconstruct the underlying geometry. Direct2.5 [55] adopts a remeshing-based technique to recover geometry from generated sparse normal maps. Another line of research involves directly mapping sparse-views into 3D representations [11, 51, 68, 81, 83, 84, 97, 103–105]. LRM [30], PF-LRM [40], and Instant3D [41] adopt a huge transformer to directly predict triplanes from single or sparse views. TriplaneGaussian [117] and LGM [85] instead map sparse views into more memory-efficient 3D Gaussian Splatting which supports much higher resolution for supervision. Our concurrent work IM-3D [56] also explores the capability of video diffusion models in object-centric multi-view generation, we further extend this paradigm in scene-level novel view synthesis and achieve better performance.

2.2 Generative Models for Novel View Synthesis

While NeRF [60] and 3D Gaussian Splatting [35] have shown impressive performance in novel view synthesis with a sufficient number of inputs, reconstruction from sparse views requires additional priors due to the incomplete information provided. Early work mainly focuses on using regression-based [12, 21, 28, 72, 90, 91, 96, 106, 111] or GAN-based [8, 9, 22, 23, 27, 62, 64, 77, 113] methods for generalizable scene reconstruction. However, due to the lack of high-quality data and the limited model capacity, the generated novel views are often blurry and exhibit poor generalization ability. Subsequent work further integrates diffusion priors to achieve better scene-level novel view synthesis [33, 100]. SparseFusion [112] proposes view-conditioned diffusion with epipolar feature transformer to synthesize

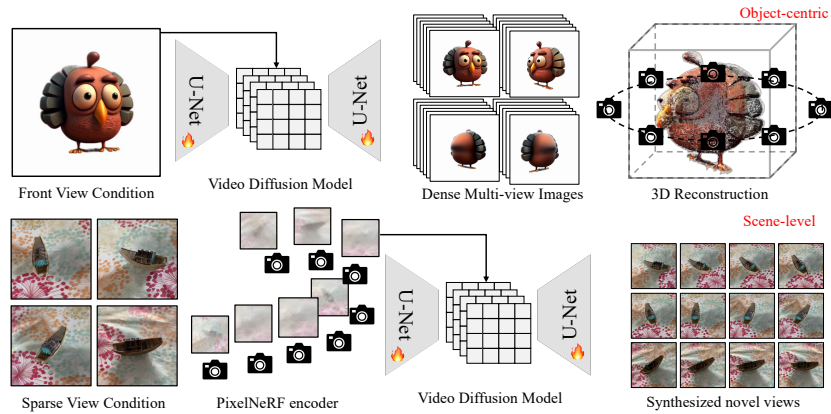


Fig. 2: Overview of the proposed V3D.

novel views with sparse inputs. GeNVS [10] utilizes a PixelNeRF encoder to incorporate geometry information and exploits an auto-aggressive generation strategy to enhance multi-view consistency. ZeroNVS [74] extends Zero-1-to-3 [49] to unbounded scenes and resolves the scale ambiguity with better camera pose conditioning. ReconFusion [102] proposes to fine-tune image diffusion models to condition on multi-view input and utilizes a novel sample loss to reconstruct the 3D scene from sparse posed inputs. We draw inspiration from ReconFusion and GeNVS, adopting PixelNeRF-based conditioner to accommodate any number of input images and provide precise camera path control in scene-level generation.

3 Approach

3.1 Overall Structure

As demonstrated in Fig. 2, the core insight of V3D lies in conceptualizing dense multi-view synthesis as video generation, thus leveraging the structure and powerful priors of the large-scale pre-trained video diffusion model to facilitate consistent multi-view generation. For object-centric image-to-3D, we fine-tune the base video diffusion model on 360° orbit videos of synthetic 3D objects rendered on fixed circular camera poses (Sec. 3.2) and design a reconstruction and mesh extraction pipeline that is tailored for generated multi-views (Sec. 3.3). For scene-level novel view synthesis, we enhance the base video diffusion model by incorporating a PixelNeRF encoder, enabling it to precisely control camera poses of generated frames and seamlessly adapt to any number of input images (Sec. 3.4). The detailed V3D methodology is presented as follows.

3.2 Dense View Prediction as Video Generation

Previous multi-view generation models [15, 89, 101] often extend from image diffusion models, incorporating multi-view cross attention (e.g. Wonder3D [52]

and Zero123-XL [79]) or intermediate 3D representations (e.g. SyncDreamer [50] with 3D voxels and Viewset Diffusion [84] and DMV3D [104] with triplane NeRF) to enhance the consistency of generated images across different views. The former tends to involve a limited number of views due to the use of cross-attention with quadratic complexity, whereas the latter often results in low image resolution due to memory-consuming 3D representations and volume rendering. To overcome these drawbacks, V3D adopts a fundamentally distinct approach to generate dense multi-view images given a single view. Inspired by Stable Video Diffusion (SVD) [4], we interpret continuous multi-view images rotating around an object as a video, thereby treating multi-view generation as a form of image-to-video generation with the front view as the condition. This approach capitalizes on the comprehensive understanding of the 3D world offered by large-scale pre-trained video diffusion models to address the scarcity of 3D data and harnesses the inherent network architecture of video diffusion models to effectively produce an adequate number of multi-view images.

Conditioning. Similar to SVD, we provide high-level semantic information of the front view by injecting the corresponding CLIP embedding into the diffusion U-Net via cross-attention and prompt the diffusion model low-level information by concatenating its latent along the channel dimension of the input. To better adapt to image-to-3D, we removed irrelevant conditions including motion bucket ID and FPS ID, and opted not to condition on elevation angle. Instead, we randomly rotate the object in elevation to make the generation model compatible with inputs with non-zero elevation. Our modification to the conditioning arises from experimental evidence suggesting that it is not feasible to perfectly constrain the elevation of generated multi-view images to a specified angle. The misalignment between the camera poses of the video and those used for reconstruction could lead to significant damage to the final outcomes.

Data. We fine-tune the base video diffusion model on the Objaverse dataset [19] for object-centric image-to-3D. It is well-established that the Objaverse dataset contains quite many low-quality 3D objects [47, 52] which may significantly degenerate the model performance [49]. We, therefore, start by manually curating a subset with higher quality, comprising approximately 290k synthetic 3D triangle meshes. We then construct a 360° orbit video dataset by rendering synthetic 3D objects in this filtered subset on $N = 18$ fixed camera poses. Specifically, for each object, we normalize the mesh to unit length, fix the camera distance to 2, set the elevation to 0, and uniformly move the camera on the azimuth N times (from 0 to 2π) to generate a smooth orbit video at 512 resolution.

Training. We follow SVD to adopt the commonly used EDM [34] framework with the simplified diffusion loss for fine-tuning. For the noise distribution used in training, we inspired by [46, 79], adopt a relatively large noise distribution with $P_{\text{mean}} = 1.5$ and $P_{\text{std}} = 2.0$. To enable classifier-free guidance, we randomly set

the latent and the CLIP embedding of the front view to zero independently with a probability of 20%. To speed up training and save GPU VRAM, we preprocess and store the latent and CLIP embedding of all video frames beforehand. During training, we load these tensors directly from the disk instead of computing them on the fly. We fine-tuned the base diffusion model for 22.5k steps, taking about one day. More detailed training settings are provided in the supplemental material.

3.3 Robust 3D Reconstruction and Mesh Extraction

After obtaining dense views of an object using the fine-tuned video diffusion model, our next step is to reconstruct the underlying 3D object from these views. While the obtained multi-view images are of high resolution and satisfactory consistency, it’s challenging to ensure strict pixel-to-pixel alignment between different views. In this case, directly applying pixel-wise loss for 3D reconstruction often leads to artifacts such as floaters or blurry textures [3, 45, 66]. In response, we propose using image-level perceptual loss to resolve inconsistencies among multiple input images. To support image-level loss, we opt for 3D Gaussian Splatting due to its fast training speed and great memory efficiency that enables rendering the full image with minimal cost. We adopt LPIPS [110] as the perceptual loss and combine it with the original loss for 3DGS, i.e.

$$\mathcal{L}_{\text{recon}}(I, I^{\text{gt}}) = \text{MSE}(I, I^{\text{gt}}) + \lambda_s \text{D-SSIM}(I, I^{\text{gt}}) + \lambda_l \text{LPIPS}(I, I^{\text{gt}}) \quad (1)$$

where I and I^{gt} represent the rendered images and the ground truth images (our generated views), λ_s and λ_l refer to the loss weights.

Initialization. Initialization is crucial for 3D Gaussian Splatting to achieve promising results [35, 115]. Due to no sparse point cloud available in object-centric reconstruction, the original 3DGS initializes the Gaussians with Gaussian-blob and removes unnecessary Gaussians by resetting opacities. This requires many optimization iterations to eliminate the floaters, and artifacts may occur when the input images are not perfectly consistent. To accelerate the reconstruction, we propose to initialize the Gaussians by space carving [38, 55]. Concretely, we first segment the foreground of the generated frames with an off-the-shelf background removal model to obtain an object mask for each view. An occupancy grid is then established by projecting voxels onto image planes to determine whether the projected pixel belongs to the object and aggregating the results of all projections under all views. Finally, we exploit marching cubes [54] to obtain a surface according to this occupancy grid and uniformly sample N_{init} points on the surface as the initializing positions of the Gaussians.

Mesh Extraction. For the demand of real-world applications, we also propose a mesh extraction pipeline for generated views. Similar to [50, 52, 88], we adopt NeuS [94] with multi-resolution hash grid [61] for fast surface reconstruction.

While V3D can generate a considerable number of views, it remains modest compared to the typical use cases of NeuS, which commonly involve more than 40 posed images [53, 94]. Therefore we adopt a normal smooth loss and a sparse regularization loss to ensure a reasonable geometry. Besides, since our generated images are not perfectly consistent and it is not feasible for NeuS to exploit image-level loss due to the high render cost, the textures of the mesh extracted by NeuS are often blurry. To address this, we further refine the texture of the NeuS extracted mesh with generated multi-views using LPIPS loss while keeping the geometry unchanged, which greatly reduces the rendering cost and enhances the quality of final outputs. Owing to the great efficiency of differentiable mesh rendering [39], this refinement process can be completed within 15 seconds.

3.4 Scene-level Novel View Synthesis

In addition to object-centric generation, we further extend video diffusion to scene-level novel view synthesis. Unlike generating views of objects, novel view synthesis entails generating images along a given camera path, which requires precise control over camera poses and accommodating multiple input images.

Conditioning. Previous approaches, such as Zero-1-to-3 [49], incorporate camera poses into image diffusion by introducing camera embeddings. However, this method did not explicitly utilize 3D information, thus making it challenging to ensure consistency across multiple views and precise control over camera pose [48, 102]. To better incorporate 3D prior into video diffusion and precisely control the poses of generated frames, we draw inspiration from GeNVS [10] and ReconFusion [102], integrating a PixelNeRF [106] feature encoder into video diffusion models. Specifically, given a set of posed images as condition $\pi_{\text{cond}}, I_{\text{cond}} = \{(I_i, \pi_i)\}_i$, we adopt a PixelNeRF to render the feature map of the target camera poses $\{\pi\}$ by:

$$f = \text{PixelNeRF}(\{\pi\} | \pi_{\text{cond}}, I_{\text{cond}}), \quad (2)$$

where $\{\pi\}$ refers to the camera poses of the frames we want to generate. We then concatenate this feature map to the input of the U-Net to explicitly encode relative camera pose information. This approach seamlessly supports an arbitrary number of images as input. Other conditionings are similar to those of object-centric generation, except that the number of CLIP image embedding has been increased from one to multiple.

Data. For scene-level novel view synthesis, we fine-tune the base video diffusion model on MVImgNet [107] which consists of 219k posed real-world video clips. To make the videos from MVImgNet compatible with the input size of the video diffusion, we obtain the object masks with an off-the-shelf background removal tool, then crop, recenter the image, and adjust the principal points and focal lengths according to the foreground mask.



Fig. 3: Qualitative comparison between the proposed V3D and state-of-the-art 3DGS-based image-to-3D methods (LGM [85] and TriplaneGaussian [117]) and optimization-based methods (Magic123 [69] and ImageDream [95]). The corresponding 360° videos are demonstrated in the supplemental video.

Training. Except for the simplified diffusion loss used in video diffusion models, we follow ReconFusion [102] to regulate the parameters of the PixelNeRF encoder with a down-sampled photometric loss:

$$\mathcal{L}_{\text{PixelNeRF}} = \mathbb{E} \| f_{\text{RGB}}(\pi | x_{\text{cond}}, \pi_{\text{cond}}) - x_{\downarrow} \| \quad (3)$$

where f_{RGB} refers to another color branch of the PixelNeRF encoder that predicts a downsampled image and x_{\downarrow} refers to the downsampled target frames.

We experimentally found this loss crucial to avoid local minima, as illustrated in [102]. We follow InstructPix2Pix [6], initializing the newly added input channels for the PixelNeRF feature in the first layer of the diffusion U-Net with zero to best keep the pre-trained priors. For input views conditioning, we randomly select 1 to 4 images as input and set the conditions to zeros independently with a probability of 20%. We present more training details of the scene-level model in the supplemental material.

4 Experiments

In this section, we present our experiments on validating the effectiveness of the proposed approach in both object-centric and scene-level 3D generation. Specifically, we quantitatively and qualitatively compare V3D with previous state-of-the-art methods in image-to-3D and novel view synthesis. Additionally, we conduct several ablation studies to evaluate the importance of model designs, including noise distribution, number of fine-tuning steps, pre-training prior, and camera conditioning. The detailed results are shown as follows.

4.1 Object-centric 3D Generation

Qualitative Comparisons. We evaluate the performance of the proposed V3D on image-to-3D and compare the results with state-of-the-art methods. The upper part of Fig. 3 demonstrates qualitative comparisons between our approach with 3DGS-based methods TriplaneGaussian [117] and LGM [85]. Our approach demonstrates impressive quality improvement, while TriplaneGaussian and LGM tend to generate a much more blurry appearance due to the limited number of Gaussians they can produce. The lower part of Fig. 3 presents a comparison between state-of-the-art SDS-based methods, including Magic123 [69] and ImageDream [95]. V3D outperforms in both front-view alignment and fidelity. In contrast, objects generated by Magic123 exhibit inaccurate geometry and blurry backface, while ImageDream tends to generate assets with over-saturated textures. Importantly, our method achieves these results within 3 minutes, making significant acceleration compared to optimization-based methods which require more than 30 minutes. Fig. 4 illustrates comparisons on multi-view generation with SyncDreamer [50] and Wonder3D [52], where our approach consistently achieves superior results with a higher resolution of 512 and much finer details. SyncDreamer tends to generate multi-view images that are simple in geometry and with over-saturated texture. We attribute this to the significant difference in structure between SyncDreamer and the original Stable Diffusion, thus failing to fully leverage the information from image pre-training. As for Wonder3D, our model triples the number of generated multi-views and doubles the resolution, achieving significant improvements in both texture quality and multi-view consistency.

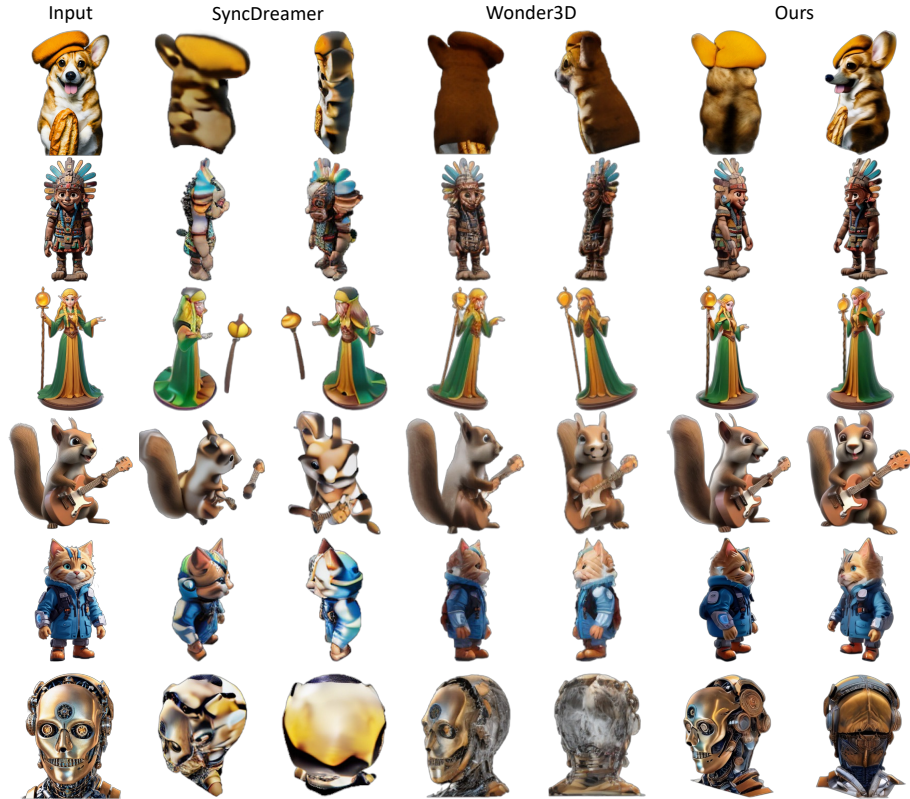


Fig. 4: Qualitative comparison of generated views between the proposed V3D and state-of-the-art multi-view generation methods, including SyncDreamer [50] and Wonder3D [52]. The corresponding 360° videos are shown in the supplemental video.

Quantitative Comparisons. For qualitative comparisons, we conduct a user study to evaluate the generated 3D assets with human ratings. Specifically, we ask 58 volunteers to evaluate objects generated by V3D and other methods under 30 condition images by watching the rendered 360° spiral videos, and choose the best method in (a) Alignment: how well does the 3D asset align with the condition image; (b) Fidelity: how realistic is the generated object. Tab. 1 demonstrates the win rate of each method in the two criteria. V3D is regarded as the most convincing model of all, and it significantly outperforms other competitors in both image alignment and fidelity.

4.2 Novel View Synthesis

For scene-level novel view synthesis, we test the performance of the proposed V3D on the 10-category subset of the CO3D dataset. To align with the settings of previous methods, we fine-tune V3D on videos in each category for only one epoch (denoted as “fine-tuned”). The results are shown in Tab. 3. Our approach

Table 1: User study results. We collect 58 anonymous preference results on image alignment and fidelity.

| Approach | Alignment Fidelity | |
|------------------------|--------------------|--------------|
| SyncDreamer [50] | 10.34 | 5.17 |
| Wonder3D [52] | 17.24 | 12.07 |
| TriplaneGaussian [117] | 6.90 | 3.45 |
| LGM [85] | 13.79 | 24.14 |
| Ours | 51.72 | 55.17 |

Table 2: Quantitative comparison of dense multi-view synthesis on Google Scanned Objects dataset [20].

| Approach | PSNR \uparrow | SSIM \uparrow | LPIPS \downarrow |
|--------------------|-----------------|-----------------|--------------------|
| RealFusion [57] | 15.26 | 0.722 | 0.283 |
| Zero-1-to-3 [49] | 18.93 | 0.779 | 0.166 |
| SyncDreamer [50] | 20.05 | 0.798 | 0.146 |
| MVDiffusion++ [88] | 21.45 | 0.844 | 0.129 |
| Ours | 22.08 | 0.882 | 0.102 |

Table 3: Quantitative comparison on 10-category subset of CO3D dataset [71]. We follow SparseFusion [112], benchmark view synthesis results with 2, 3, and 6 input views. The best result is highlighted in **bold**, while the second-best result is underscored.

| | 2 Views | | | 3 Views | | | 6 Views | | |
|---------------------------------|-----------------|-----------------|--------------------|-----------------|-----------------|--------------------|-----------------|-----------------|--------------------|
| | PSNR \uparrow | SSIM \uparrow | LPIPS \downarrow | PSNR \uparrow | SSIM \uparrow | LPIPS \downarrow | PSNR \uparrow | SSIM \uparrow | LPIPS \downarrow |
| PixelNeRF [106] | 19.52 | 0.667 | 0.327 | 20.67 | 0.712 | 0.293 | 22.47 | 0.776 | 0.241 |
| NerFormer [71] | 17.88 | 0.598 | 0.382 | 18.54 | 0.618 | 0.367 | 19.99 | 0.661 | 0.332 |
| ViewFormer [37] | 18.37 | 0.697 | 0.282 | 18.91 | 0.704 | 0.275 | 19.72 | 0.717 | 0.266 |
| EFT [26, 112] | 20.85 | 0.680 | 0.289 | <u>22.71</u> | 0.747 | 0.262 | <u>24.57</u> | 0.804 | 0.210 |
| VLDM [112] | 19.55 | 0.711 | 0.247 | 20.85 | 0.737 | 0.225 | 22.35 | 0.768 | 0.201 |
| SparseFusion [112] | <u>21.34</u> | <u>0.752</u> | 0.225 | 22.35 | 0.766 | 0.216 | 23.74 | 0.791 | 0.200 |
| Ours (w. camera emb.) | 18.27 | 0.598 | 0.303 | 18.83 | 0.605 | 0.273 | - | - | - |
| Ours (w. Plücker emb.) | 20.11 | 0.714 | 0.277 | 20.39 | 0.727 | 0.223 | - | - | - |
| Ours (w/o. pre-training) | 16.20 | 0.544 | 0.333 | 16.76 | 0.576 | 0.303 | - | - | - |
| Ours (zero-shot) | 20.64 | 0.734 | <u>0.213</u> | 22.04 | 0.805 | <u>0.141</u> | 23.94 | <u>0.851</u> | <u>0.126</u> |
| Ours (fine-tuned) | 22.19 | 0.790 | 0.093 | 23.31 | 0.860 | 0.082 | 24.70 | 0.890 | 0.074 |

achieves consistently better performance in terms of image metrics against previous state-of-the-art novel view synthesizers by a clear margin, demonstrating the effectiveness of utilizing pre-trained video diffusion models in scene-level novel view synthesis. Besides, V3D shows impressive generalization ability as the zero-shot version of V3D (only trained on MVImgNet) beats most of the competitors.

Qualitative Comparisons. We show in Fig. 5 qualitative comparisons on generated multi-views between SparseFusion [112] on the *hydrant* subset of the CO3D dataset [71]. For better comparison, we use COLMAP [75, 76] to perform multi-view stereo reconstruction given camera poses and showcased, in Fig. 5, the number of points in the obtained point cloud and the Chamfer distance between the one reconstructed from ground truth images. The point clouds reconstructed from V3D generated images contain more points and are closer to the point clouds reconstructed from real images. This indicates a significant advantage of our method in terms of both reconstruction quality and multi-view consistency.

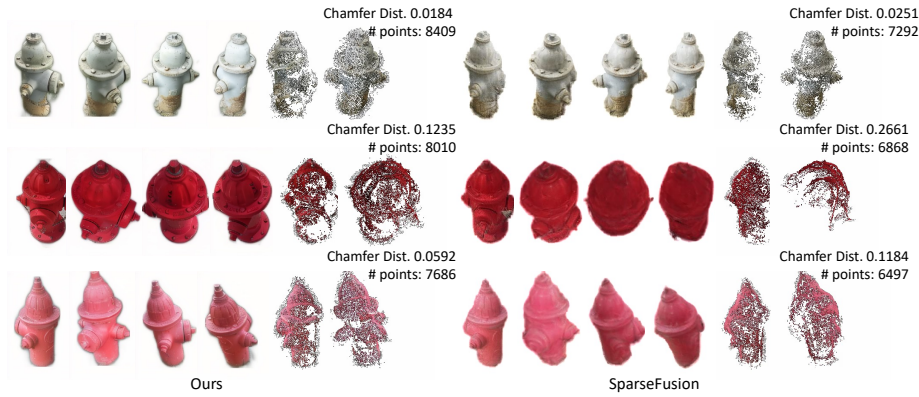


Fig. 5: Qualitative comparison on scene-level novel view synthesis with SparseFusion on *hydrant* subset of CO3D dataset. We reconstruct a sparse point cloud using COLMAP and report the number of points and Chamfer distance against the point cloud extracted with ground truth images.

4.3 Ablations

Pre-training. To demonstrate the impact of large-scale video pre-training, we trained a variant of the model from scratch on the constructed Objaverse 360° orbit video for 45k steps, which, apart from the initialized weights of the diffusion U-Net, is identical to the full model. As shown in Fig. 6, this from-scratch variant completely failed to generate multi-view images even with doubled training steps compared to the full model, demonstrating the significant importance of adopting large-scale video pre-training.

Number of Fine-tuning Steps. To illustrate the impact of the Objaverse dataset on the pre-trained model, we fine-tune the base model with different training steps, as shown in the top part of Fig. 6. Due to the considerably lower complexity of renders from Objaverse objects, excessive fine-tuning steps can yield overly simplistic textures in the generated frames, while an inadequate number of fine-tuning steps may lead to strange and inaccurate geometries.

Noise Distribution. To validate the necessity of adopting a large noise distribution during training, we fine-tune the base diffusion model with a smaller noise schedule ($P_{\text{mean}} = 0.7$ and $P_{\text{std}} = 1.6$), which is used in the image-to-video pre-training in Stable Video Diffusion. As demonstrated in the lower part of Fig. 6, the model trained with a smaller noise distribution tends to generate geometric structures that are unreasonable (the pistol) or degenerated (the cartoon-style astronaut). We attribute this phenomenon to the strong image signal we exploited and the relatively simple nature of the synthetic Objaverse dataset, indicating the need to shift the noise distribution towards stronger noise.

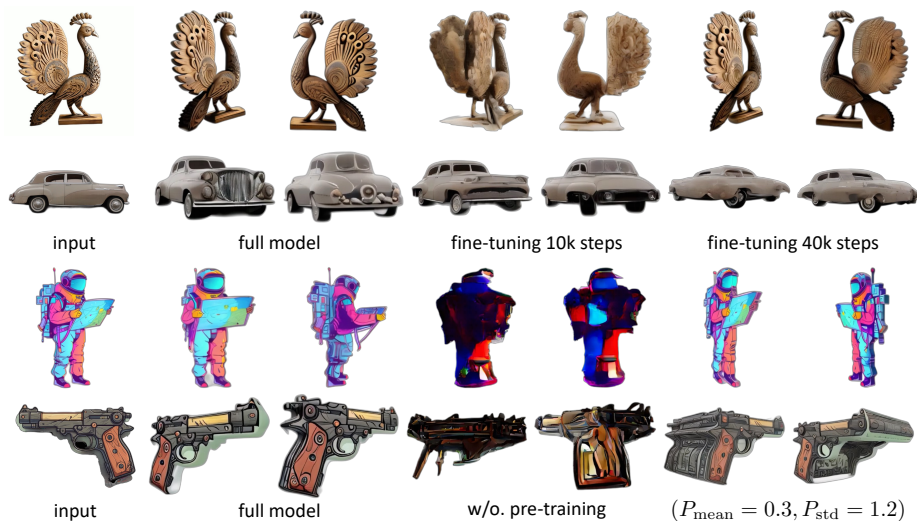


Fig. 6: Ablations study. We show that the number of fine-tuning steps, large-scale pre-training, and stronger noise distribution are crucial for achieving promising results.

Camera Conditioning. To assess the impact of the approach of camera conditioning, we introduce two variants that condition on camera poses by commonly used learnable camera embedding or the Plücker ray embedding. For a fair comparison, for both variants, we additionally concatenate the multi-view images used as conditions into the input of the diffusion U-Net and similarly set the weights of added channels to zero to minimize the gap. As shown in Tab. 3, either camera embedding or Plücker embedding provides accurate 3D information and results in a significant degeneration in model performance.

5 Limitations and Conclusion

Limitations. Although achieves state-of-the-art performance in 3D generation, V3D would produce unsatisfying results for some complex objects or scenes, such as inconsistency among multiple views or unreasonable geometries. Concrete failure cases and analyses are discussed in the supplemental material.

Conclusion. In this paper, we propose V3D, a novel method for generating consistent multi-view images with image-to-video diffusion models. By fine-tuning the base video diffusion model on 3D datasets, we extend video diffusion models to effective 3D generators. Specifically, for object-centric 3D generation, we fine-tune the video diffusion on synthesizing 360° videos of 3D objects to predict dense views given a single image. To obtain the underlying 3D asset from generated views, we propose a tailored reconstruction pipeline with designed initialization and texture refinement, enabling the reconstruction of high-quality

3D Gaussians or delicate textured meshes within 3 minutes. We further extend our framework to scene-level novel view synthesis, achieving precise control over the camera path with great multi-view consistency. We conduct extensive experiments to validate the effectiveness of the proposed approach, illustrating its remarkable performance in generating consistent multi-views and generalization ability. We hope our method can serve as an efficient and powerful approach for high-quality 3D generation and could pave the way for more extensive applications of video diffusion models in 3D tasks.

References

1. Armandpour, M., Zheng, H., Sadeghian, A., Sadeghian, A., Zhou, M.: Re-imagine the negative prompt algorithm: Transform 2d diffusion into 3d, alleviate janus problem and beyond. arXiv preprint arXiv:2304.04968 (2023)
2. Bar-Tal, O., Chefer, H., Tov, O., Herrmann, C., Paiss, R., Zada, S., Ephrat, A., Hur, J., Li, Y., Michaeli, T., Wang, O., Sun, D., Dekel, T., Mosseri, I.: Lumiere: A space-time diffusion model for video generation. arXiv preprint arXiv: 2401.12945 (2024)
3. Barron, J.T., Mildenhall, B., Tancik, M., Hedman, P., Martin-Brualla, R., Srinivasan, P.P.: Mip-nerf: A multiscale representation for anti-aliasing neural radiance fields. In: Proceedings of the IEEE/CVF International Conference on Computer Vision. pp. 5855–5864 (2021)
4. Blattmann, A., Dockhorn, T., Kulal, S., Mendelevitch, D., Kilian, M., Lorenz, D.: Stable video diffusion: Scaling latent video diffusion models to large datasets. ArXiv [abs/2311.15127](https://arxiv.org/abs/2311.15127) (2023), <https://api.semanticscholar.org/CorpusID:265312551>
5. Blattmann, A., Rombach, R., Ling, H., Dockhorn, T., Kim, S.W., Fidler, S., Kreis, K.: Align your latents: High-resolution video synthesis with latent diffusion models. In: IEEE Conference on Computer Vision and Pattern Recognition (CVPR) (2023)
6. Brooks, T., Holynski, A., Efros, A.A.: Instructpix2pix: Learning to follow image editing instructions. In: CVPR (2023)
7. Brooks, T., Peebles, B., Holmes, C., DePue, W., Guo, Y., Jing, L., Schnurr, D., Taylor, J., Luhman, T., Luhman, E., Ng, C., Wang, R., Ramesh, A.: Video generation models as world simulators (2024), <https://openai.com/research/video-generation-models-as-world-simulators>
8. Chan, E., Lin, C.Z., Chan, M., Nagano, K., Pan, B., Mello, S.D., Gallo, O., Guibas, L.J., Tremblay, J., Khamis, S., Karras, T., Wetzstein, G.: Efficient geometry-aware 3d generative adversarial networks. 2022 IEEE/CVF Conference on Computer Vision and Pattern Recognition (CVPR) pp. 16102–16112 (2021), <https://api.semanticscholar.org/CorpusID:245144673>
9. Chan, E., Monteiro, M., Kellnhofer, P., Wu, J., Wetzstein, G.: pi-gan: Periodic implicit generative adversarial networks for 3d-aware image synthesis. In: arXiv (2020)
10. Chan, E.R., Nagano, K., Chan, M.A., Bergman, A.W., Park, J.J., Levy, A., Ait-tala, M., Mello, S.D., Karras, T., Wetzstein, G.: GeNVS: Generative novel view synthesis with 3D-aware diffusion models. In: arXiv (2023)
11. Charatan, D., Li, S., Tagliasacchi, A., Sitzmann, V.: pixelsplat: 3d gaussian splats from image pairs for scalable generalizable 3d reconstruction. arXiv preprint arXiv: 2312.12337 (2023)
12. Chen, A., Xu, Z., Zhao, F., Zhang, X., Xiang, F., Yu, J., Su, H.: Mvsnerf: Fast generalizable radiance field reconstruction from multi-view stereo. 2021 IEEE/CVF International Conference on Computer Vision (ICCV) pp. 14104–14113 (2021), <https://api.semanticscholar.org/CorpusID:232404617>
13. Chen, H., Zhang, Y., Cun, X., Xia, M., Wang, X., Weng, C., Shan, Y.: Videocrafter2: Overcoming data limitations for high-quality video diffusion models (2024)
14. Chen, R., Chen, Y., Jiao, N., Jia, K.: Fantasia3d: Disentangling geometry and appearance for high-quality text-to-3d content creation. In: Proceedings of the IEEE/CVF International Conference on Computer Vision (ICCV) (October 2023)

15. Chen, Y., Fang, J., Huang, Y., Yi, T., Zhang, X., Xie, L., Wang, X., Dai, W., Xiong, H., Tian, Q.: Cascade-zero123: One image to highly consistent 3d with self-prompted nearby views. ArXiv **abs/2312.04424** (2023), <https://api.semanticscholar.org/CorpusID:266051982>
16. Chen, Y., Chen, Z., Zhang, C., Wang, F., Yang, X., Wang, Y., Cai, Z., Yang, L., Liu, H., Lin, G.: Gaussianeditor: Swift and controllable 3d editing with gaussian splatting. CoRR **abs/2311.14521** (2023). <https://doi.org/10.48550/ARXIV.2311.14521>, <https://doi.org/10.48550/arXiv.2311.14521>
17. Chen, Y., Chen, R., Lei, J., Zhang, Y., Jia, K.: TANGO: text-driven photorealistic and robust 3d stylization via lighting decomposition. In: NeurIPS (2022), http://papers.nips.cc/paper_files/paper/2022/hash/c7b925e600ae4880f5c5d7557f70a72b-Abstract-Conference.html
18. Chen, Z., Wang, F., Wang, Y., Liu, H.: Text-to-3d using gaussian splatting. In: CVPR (2024), <https://arxiv.org/abs/2309.16585>
19. Deitke, M., Schwenk, D., Salvador, J., Weihs, L., Michel, O., VanderBilt, E., Schmidt, L., Ehsani, K., Kembhavi, A., Farhadi, A.: Objaverse: A universe of annotated 3d objects. arXiv preprint arXiv:2212.08051 (2022)
20. Downs, L., Francis, A., Koenig, N., Kinman, B., Hickman, R.M., Reymann, K., McHugh, T.B., Vanhoucke, V.: Google scanned objects: A high-quality dataset of 3d scanned household items. 2022 International Conference on Robotics and Automation (ICRA) pp. 2553–2560 (2022), <https://api.semanticscholar.org/CorpusID:248392390>
21. Flynn, J., Neulander, I., Philbin, J., Snavely, N.: Deep stereo: Learning to predict new views from the world’s imagery. 2016 IEEE Conference on Computer Vision and Pattern Recognition (CVPR) pp. 5515–5524 (2015), <https://api.semanticscholar.org/CorpusID:14517241>
22. Gadelha, M., Maji, S., Wang, R.: 3d shape induction from 2d views of multiple objects. 2017 International Conference on 3D Vision (3DV) pp. 402–411 (2016), <https://api.semanticscholar.org/CorpusID:2516262>
23. Gao, J., Shen, T., Wang, Z., Chen, W., Yin, K., Li, D., Litany, O., Gojcic, Z., Fidler, S.: Get3d: A generative model of high quality 3d textured shapes learned from images. ArXiv **abs/2209.11163** (2022), <https://api.semanticscholar.org/CorpusID:252438648>
24. Girdhar, R., Singh, M., Brown, A., Duval, Q., Azadi, S., Rambhatla, S.S., Shah, A., Yin, X., Parikh, D., Misra, I.: Emu video: Factorizing text-to-video generation by explicit image conditioning. arXiv preprint arXiv: 2311.10709 (2023)
25. Guo, Y., Yang, C., Rao, A., Liang, Z., Wang, Y., Qiao, Y., Agrawala, M., Lin, D., Dai, B.: Animatediff: Animate your personalized text-to-image diffusion models without specific tuning (2023)
26. He, Y., Yan, R., Fragkiadaki, K., Yu, S.I.: Epipolar transformers. 2020 IEEE/CVF Conference on Computer Vision and Pattern Recognition (CVPR) pp. 7776–7785 (2020), <https://api.semanticscholar.org/CorpusID:218581558>
27. Henzler, P., Mitra, N.J., Ritschel, T.: Escaping plato’s cave: 3d shape from adversarial rendering. 2019 IEEE/CVF International Conference on Computer Vision (ICCV) pp. 9983–9992 (2018), <https://api.semanticscholar.org/CorpusID:207976631>
28. Henzler, P., Reizenstein, J., Labatut, P., Shapovalov, R., Ritschel, T., Vedaldi, A., Novotný, D.: Unsupervised learning of 3d object categories from videos in the wild. 2021 IEEE/CVF Conference on Computer Vision and Pattern Recognition (CVPR) pp. 4698–4707 (2021), <https://api.semanticscholar.org/CorpusID:232417771>

29. Hertz, A., Aberman, K., Cohen-Or, D.: Delta denoising score. In: IEEE/CVF International Conference on Computer Vision, ICCV 2023, Paris, France, October 1-6, 2023. pp. 2328–2337. IEEE (2023). <https://doi.org/10.1109/ICCV51070.2023.00221>, <https://doi.org/10.1109/ICCV51070.2023.00221>
30. Hong, Y., Zhang, K., Gu, J., Bi, S., Zhou, Y., Liu, D., Liu, F., Sunkavalli, K., Bui, T., Tan, H.: LRM: large reconstruction model for single image to 3d. CoRR **abs/2311.04400** (2023). <https://doi.org/10.48550/ARXIV.2311.04400>, <https://doi.org/10.48550/arXiv.2311.04400>
31. Jain, A., Mildenhall, B., Barron, J.T., Abbeel, P., Poole, B.: Zero-shot text-guided object generation with dream fields. In: IEEE/CVF Conference on Computer Vision and Pattern Recognition, CVPR 2022, New Orleans, LA, USA, June 18-24, 2022. pp. 857–866. IEEE (2022). <https://doi.org/10.1109/CVPR52688.2022.00094>, <https://doi.org/10.1109/CVPR52688.2022.00094>
32. Jun, H., Nichol, A.: Shap-e: Generating conditional 3d implicit functions. CoRR **abs/2305.02463** (2023). <https://doi.org/10.48550/arXiv.2305.02463>, <https://doi.org/10.48550/arXiv.2305.02463>
33. Karnewar, A., Vedaldi, A., Novotny, D., Mitra, N.: Holodiffusion: Training a 3D diffusion model using 2D images. In: Proceedings of the IEEE/CVF conference on computer vision and pattern recognition (2023)
34. Karras, T., Aittala, M., Aila, T., Laine, S.: Elucidating the design space of diffusion-based generative models. In: Proc. NeurIPS (2022)
35. Kerbl, B., Kopanas, G., Leimkühler, T., Drettakis, G.: 3d gaussian splatting for real-time radiance field rendering. ACM Transactions on Graphics **42**(4) (July 2023), <https://repo-sam.inria.fr/fungraph/3d-gaussian-splatting/>
36. Khalid, N.M., Xie, T., Belilovsky, E., Tiberiu, P.: Clip-mesh: Generating textured meshes from text using pretrained image-text models. SIGGRAPH Asia 2022 Conference Papers (December 2022)
37. Kulhánek, J., Derner, E., Sattler, T., Babuška, R.: Viewformer: Nerf-free neural rendering from few images using transformers. In: European Conference on Computer Vision (ECCV) (2022)
38. Kutulakos, K.N., Seitz, S.M.: A theory of shape by space carving. International Journal of Computer Vision **38**, 199–218 (1999), <https://api.semanticscholar.org/CorpusID:1538200>
39. Laine, S., Hellsten, J., Karras, T., Seol, Y., Lehtinen, J., Aila, T.: Modular primitives for high-performance differentiable rendering. ACM Transactions on Graphics **39**(6) (2020)
40. Li, J., Tan, H., Zhang, K., Xu, Z., Luan, F., Xu, Y., Hong, Y., Sunkavalli, K., Shakhnarovich, G., Bi, S.: Instant3d: Fast text-to-3d with sparse-view generation and large reconstruction model. CoRR **abs/2311.06214** (2023). <https://doi.org/10.48550/ARXIV.2311.06214>, <https://doi.org/10.48550/arXiv.2311.06214>
41. Li, J., Tan, H., Zhang, K., Xu, Z., Luan, F., Xu, Y., Hong, Y., Sunkavalli, K., Shakhnarovich, G., Bi, S.: Instant3d: Fast text-to-3d with sparse-view generation and large reconstruction model. CoRR **abs/2311.06214** (2023). <https://doi.org/10.48550/ARXIV.2311.06214>, <https://doi.org/10.48550/arXiv.2311.06214>
42. Li, W., Chen, R., Chen, X., Tan, P.: Sweetdreamer: Aligning geometric priors in 2d diffusion for consistent text-to-3d. arxiv:2310.02596 (2023)
43. Li, X., Zhou, D., Zhang, C., Wei, S., Hou, Q., Cheng, M.M.: Sora generates videos with stunning geometrical consistency. arXiv preprint arXiv: 2402.17403 (2024)

44. Lin, C.H., Gao, J., Tang, L., Takikawa, T., Zeng, X., Huang, X., Kreis, K., Fidler, S., Liu, M.Y., Lin, T.Y.: Magic3d: High-resolution text-to-3d content creation. In: IEEE Conference on Computer Vision and Pattern Recognition (CVPR) (2023)
45. Lin, C.H., Ma, W.C., Torralba, A., Lucey, S.: Barf: Bundle-adjusting neural radiance fields. In: IEEE International Conference on Computer Vision (ICCV) (2021)
46. Lin, S., Liu, B., Li, J., Yang, X.: Common diffusion noise schedules and sample steps are flawed. ArXiv [abs/2305.08891](https://arxiv.org/abs/2305.08891) (2023), <https://api.semanticscholar.org/CorpusID:258714883>
47. Liu, M., Shi, R., Chen, L., Zhang, Z., Xu, C., Wei, X., Chen, H., Zeng, C., Gu, J., Su, H.: One-2-3-45++: Fast single image to 3d objects with consistent multi-view generation and 3d diffusion. arXiv preprint [arXiv:2311.07885](https://arxiv.org/abs/2311.07885) (2023)
48. Liu, M., Xu, C., Jin, H., Chen, L., Xu, Z., Su, H., et al.: One-2-3-45: Any single image to 3d mesh in 45 seconds without per-shape optimization. arXiv preprint [arXiv:2306.16928](https://arxiv.org/abs/2306.16928) (2023)
49. Liu, R., Wu, R., Hoorick, B.V., Tokmakov, P., Zakharov, S., Vondrick, C.: Zero-1-to-3: Zero-shot one image to 3d object. <https://arxiv.org/abs/2303.11328> (2023)
50. Liu, Y., Lin, C., Zeng, Z., Long, X., Liu, L., Komura, T., Wang, W.: Syncdreamer: Generating multiview-consistent images from a single-view image. arXiv preprint [arXiv:2309.03453](https://arxiv.org/abs/2309.03453) (2023)
51. Liu, Z., Li, Y., Lin, Y., Yu, X., Peng, S., Cao, Y.P., Qi, X., Huang, X., Liang, D., Ouyang, W.: Unidream: Unifying diffusion priors for relightable text-to-3d generation (2023)
52. Long, X., Guo, Y.C., Lin, C., Liu, Y., Dou, Z., Liu, L., Ma, Y., Zhang, S.H., Habermann, M., Theobalt, C., et al.: Wonder3d: Single image to 3d using cross-domain diffusion. arXiv preprint [arXiv:2310.15008](https://arxiv.org/abs/2310.15008) (2023)
53. Long, X., Lin, C.H., Wang, P., Komura, T., Wang, W.: Sparseneus: Fast generalizable neural surface reconstruction from sparse views. ArXiv [abs/2206.05737](https://arxiv.org/abs/2206.05737) (2022), <https://api.semanticscholar.org/CorpusID:249625516>
54. Lorensen, W.E., Cline, H.E.: Marching cubes: A high resolution 3d surface construction algorithm. Proceedings of the 14th annual conference on Computer graphics and interactive techniques (1987), <https://api.semanticscholar.org/CorpusID:15545924>
55. Lu, Y., Zhang, J., Li, S., Fang, T., McKinnon, D., Tsin, Y., Quan, L., Cao, X., Yao, Y.: Direct2.5: Diverse text-to-3d generation via multi-view 2.5d diffusion. ArXiv [abs/2311.15980](https://arxiv.org/abs/2311.15980) (2023), <https://api.semanticscholar.org/CorpusID:265456029>
56. Melas-Kyriazi, L., Laina, I., Rupperecht, C., Neverova, N.V., Vedaldi, A., Gafni, O., Kokkinos, F.: Im-3d: Iterative multiview diffusion and reconstruction for high-quality 3d generation. ArXiv [abs/2402.08682](https://arxiv.org/abs/2402.08682) (2024), <https://api.semanticscholar.org/CorpusID:267636572>
57. Melas-Kyriazi, L., Rupperecht, C., Laina, I., Vedaldi, A.: Realfusion: 360 reconstruction of any object from a single image. In: CVPR (2023), <https://arxiv.org/abs/2302.10663>
58. Metzger, G., Richardson, E., Patashnik, O., Giryes, R., Cohen-Or, D.: Latentnerf for shape-guided generation of 3d shapes and textures. arXiv preprint [arXiv:2211.07600](https://arxiv.org/abs/2211.07600) (2022)
59. Michel, O., Bar-On, R., Liu, R., Benaim, S., Hanocka, R.: Text2mesh: Text-driven neural stylization for meshes. In: IEEE/CVF Conference on Computer Vision and Pattern Recognition, CVPR 2022, New Orleans, LA, USA, June 18-24, 2022. pp.

- 13482–13492. IEEE (2022). <https://doi.org/10.1109/CVPR52688.2022.01313>, <https://doi.org/10.1109/CVPR52688.2022.01313>
60. Mildenhall, B., Srinivasan, P.P., Tancik, M., Barron, J.T., Ramamoorthi, R., Ng, R.: Nerf: Representing scenes as neural radiance fields for view synthesis. In: ECCV (2020)
 61. Müller, T., Evans, A., Schied, C., Keller, A.: Instant neural graphics primitives with a multiresolution hash encoding. *ACM Trans. Graph.* **41**(4), 102:1–102:15 (Jul 2022). <https://doi.org/10.1145/3528223.3530127>, <https://doi.org/10.1145/3528223.3530127>
 62. Nguyen-Phuoc, T., Li, C., Theis, L., Richardt, C., Yang, Y.L.: Hologan: Unsupervised learning of 3d representations from natural images. 2019 IEEE/CVF International Conference on Computer Vision Workshop (ICCVW) pp. 2037–2040 (2019), <https://api.semanticscholar.org/CorpusID:91184364>
 63. Nichol, A., Jun, H., Dhariwal, P., Mishkin, P., Chen, M.: Point-e: A system for generating 3d point clouds from complex prompts. *CoRR* **abs/2212.08751** (2022). <https://doi.org/10.48550/arXiv.2212.08751>, <https://doi.org/10.48550/arXiv.2212.08751>
 64. Niemeyer, M., Geiger, A.: Giraffe: Representing scenes as compositional generative neural feature fields. 2021 IEEE/CVF Conference on Computer Vision and Pattern Recognition (CVPR) pp. 11448–11459 (2020), <https://api.semanticscholar.org/CorpusID:227151657>
 65. Park, J., Kwon, G., Ye, J.C.: Ed-nerf: Efficient text-guided editing of 3d scene using latent space nerf. *CoRR* **abs/2310.02712** (2023). <https://doi.org/10.48550/ARXIV.2310.02712>, <https://doi.org/10.48550/arXiv.2310.02712>
 66. Park, K., Henzler, P., Mildenhall, B., Barron, J.T., Martin-Brualla, R.: Camp: Camera preconditioning for neural radiance fields. *ACM Transactions on Graphics (TOG)* **42**, 1 – 11 (2023), <https://api.semanticscholar.org/CorpusID:261064934>
 67. Poole, B., Jain, A., Barron, J.T., Mildenhall, B.: Dreamfusion: Text-to-3d using 2d diffusion. In: The Eleventh International Conference on Learning Representations, ICLR 2023, Kigali, Rwanda, May 1-5, 2023. OpenReview.net (2023), <https://openreview.net/pdf?id=FjNys5c7VyY>
 68. Qian, G., Cao, J., Siarohin, A., Kant, Y., Wang, C., Vasilkovsky, M., Lee, H.Y., Fang, Y., Skorokhodov, I., Zhuang, P., Gilitschenski, I., Ren, J., Ghanem, B., Aberman, K., Tulyakov, S.: Atom: Amortized text-to-mesh using 2d diffusion. arXiv preprint arXiv: 2402.00867 (2024)
 69. Qian, G., Mai, J., Hamdi, A., Ren, J., Siarohin, A., Li, B., Lee, H.Y., Skorokhodov, I., Wonka, P., Tulyakov, S., Ghanem, B.: Magic123: One image to high-quality 3d object generation using both 2d and 3d diffusion priors. In: The Twelfth International Conference on Learning Representations (ICLR) (2024), <https://openreview.net/forum?id=0jHkUDyE09>
 70. Radford, A., Kim, J.W., Hallacy, C., Ramesh, A., Goh, G., Agarwal, S., Sastry, G., Askell, A., Mishkin, P., Clark, J., Krueger, G., Sutskever, I.: Learning transferable visual models from natural language supervision. In: Meila, M., Zhang, T. (eds.) Proceedings of the 38th International Conference on Machine Learning, ICML 2021, 18-24 July 2021, Virtual Event. Proceedings of Machine Learning Research, vol. 139, pp. 8748–8763. PMLR (2021), <http://proceedings.mlr.press/v139/radford21a.html>
 71. Reizenstein, J., Shapovalov, R., Henzler, P., Sbordone, L., Labatut, P., Novotny, D.: Common objects in 3d: Large-scale learning and evaluation of real-life 3d category reconstruction. In: International Conference on Computer Vision (2021)

72. Sajjadi, M.S.M., Meyer, H., Pot, E., Bergmann, U., Greff, K., Radwan, N., Vora, S., Lucic, M., Duckworth, D., Dosovitskiy, A., Uszkoreit, J., Funkhouser, T.A., Tagliasacchi, A.: Scene representation transformer: Geometry-free novel view synthesis through set-latent scene representations. In: IEEE/CVF Conference on Computer Vision and Pattern Recognition, CVPR 2022, New Orleans, LA, USA, June 18-24, 2022. pp. 6219–6228. IEEE (2022). <https://doi.org/10.1109/CVPR52688.2022.00613>, <https://doi.org/10.1109/CVPR52688.2022.00613>
73. Sanghi, A., Chu, H., Lambourne, J.G., Wang, Y., Cheng, C.Y., Fumero, M.: Clip-forge: Towards zero-shot text-to-shape generation. arXiv preprint arXiv:2110.02624 (2021)
74. Sargent, K., Li, Z., Shah, T., Herrmann, C., Yu, H.X., Zhang, Y., Chan, E.R., Lagun, D., Fei-Fei, L., Sun, D., Wu, J.: ZeroNVS: Zero-shot 360-degree view synthesis from a single real image. arXiv preprint arXiv:2310.17994 (2023)
75. Schönberger, J.L., Frahm, J.M.: Structure-from-motion revisited. In: Conference on Computer Vision and Pattern Recognition (CVPR) (2016)
76. Schönberger, J.L., Zheng, E., Pollefeys, M., Frahm, J.M.: Pixelwise view selection for unstructured multi-view stereo. In: European Conference on Computer Vision (ECCV) (2016)
77. Schwarz, K., Sauer, A., Niemeyer, M., Liao, Y., Geiger, A.: Voxgraf: Fast 3d-aware image synthesis with sparse voxel grids. ArXiv [abs/2206.07695](https://arxiv.org/abs/2206.07695) (2022), <https://api.semanticscholar.org/CorpusID:249674609>
78. Seo, J., Jang, W., Kwak, M.S., Ko, J., Kim, H., Kim, J., Kim, J.H., Lee, J., Kim, S.: Let 2d diffusion model know 3d-consistency for robust text-to-3d generation. arXiv preprint arXiv:2303.07937 (2023)
79. Shi, R., Chen, H., Zhang, Z., Liu, M., Xu, C., Wei, X., Chen, L., Zeng, C., Su, H.: Zero123++: a single image to consistent multi-view diffusion base model (2023)
80. Shi, Y., Wang, P., Ye, J., Mai, L., Li, K., Yang, X.: Mvdream: Multi-view diffusion for 3d generation. arXiv:2308.16512 (2023)
81. Siddiqui, Y., Alliegro, A., Artemov, A., Tommasi, T., Sirigatti, D., Rosov, V., Dai, A., Nießner, M.: Meshgpt: Generating triangle meshes with decoder-only transformers. CoRR [abs/2311.15475](https://arxiv.org/abs/2311.15475) (2023). <https://doi.org/10.48550/ARXIV.2311.15475>, <https://doi.org/10.48550/arXiv.2311.15475>
82. Sun, J., Zhang, B., Shao, R., Wang, L., Liu, W., Xie, Z., Liu, Y.: Dreamcraft3d: Hierarchical 3d generation with bootstrapped diffusion prior. arXiv preprint arXiv:2310.16818 (2023)
83. Szymanowicz, S., Rupperecht, C., Vedaldi, A.: Splatter image: Ultra-fast single-view 3d reconstruction. In: arXiv (2023)
84. Szymanowicz, S., Rupperecht, C., Vedaldi, A.: Viewset diffusion: (0-)image-conditioned 3D generative models from 2D data. In: ICCV (2023)
85. Tang, J., Chen, Z., Chen, X., Wang, T., Zeng, G., Liu, Z.: Lgm: Large multi-view gaussian model for high-resolution 3d content creation. arXiv preprint arXiv:2402.05054 (2024)
86. Tang, J., Ren, J., Zhou, H., Liu, Z., Zeng, G.: Dreamgaussian: Generative gaussian splatting for efficient 3d content creation. arXiv preprint arXiv:2309.16653 (2023)
87. Tang, J., Wang, T., Zhang, B., Zhang, T., Yi, R., Ma, L., Chen, D.: Make-it-3d: High-fidelity 3d creation from a single image with diffusion prior (2023)
88. Tang, S., Chen, J., Wang, D., Tang, C., Zhang, F., Fan, Y., Chandra, V., Furukawa, Y., Ranjan, R.: Mvdifffusion++: A dense high-resolution multi-view diffusion model for single or sparse-view 3d object reconstruction. arXiv preprint arXiv:2402.12712 (2024)

89. Tang, S., Zhang, F., Chen, J., Wang, P., Yasutaka, F.: Mvdifusion: Enabling holistic multi-view image generation with correspondence-aware diffusion. arXiv preprint 2307.01097 (2023)
90. Trevithick, A., Yang, B.: Grf: Learning a general radiance field for 3d representation and rendering. 2021 IEEE/CVF International Conference on Computer Vision (ICCV) pp. 15162–15172 (2020), <https://api.semanticscholar.org/CorpusID:236975860>
91. Tucker, R., Snavely, N.: Single-view view synthesis with multiplane images. 2020 IEEE/CVF Conference on Computer Vision and Pattern Recognition (CVPR) pp. 548–557 (2020), <https://api.semanticscholar.org/CorpusID:216080881>
92. Wang, C., Chai, M., He, M., Chen, D., Liao, J.: Clip-nerf: Text-and-image driven manipulation of neural radiance fields. In: IEEE/CVF Conference on Computer Vision and Pattern Recognition, CVPR 2022, New Orleans, LA, USA, June 18–24, 2022. pp. 3825–3834. IEEE (2022). <https://doi.org/10.1109/CVPR52688.2022.00381>, <https://doi.org/10.1109/CVPR52688.2022.00381>
93. Wang, P., Xu, D., Fan, Z., Wang, D., Mohan, S., Iandola, F., Ranjan, R., Li, Y., Liu, Q., Wang, Z., Chandra, V.: Taming mode collapse in score distillation for text-to-3d generation. arXiv preprint: 2401.00909 (2023)
94. Wang, P., Liu, L., Liu, Y., Theobalt, C., Komura, T., Wang, W.: Neus: Learning neural implicit surfaces by volume rendering for multi-view reconstruction. ArXiv [abs/2106.10689](https://api.semanticscholar.org/abs/2106.10689) (2021), <https://api.semanticscholar.org/CorpusID:235490453>
95. Wang, P., Shi, Y.: Imagedream: Image-prompt multi-view diffusion for 3d generation. arXiv preprint arXiv:2312.02201 (2023)
96. Wang, Q., Wang, Z., Genova, K., Srinivasan, P.P., Zhou, H., Barron, J.T., Martin-Brualla, R., Snavely, N., Funkhouser, T.A.: Ibrnet: Learning multi-view image-based rendering. In: IEEE Conference on Computer Vision and Pattern Recognition, CVPR 2021, virtual, June 19–25, 2021. pp. 4690–4699. Computer Vision Foundation / IEEE (2021). <https://doi.org/10.1109/CVPR46437.2021.00466>, https://openaccess.thecvf.com/content/CVPR2021/html/Wang_IBRNet_Learning_Multi-View_Image-Based_Rendering_CVPR_2021_paper.html
97. Wang, T., Zhang, B., Zhang, T., Gu, S., Bao, J., Baltrusaitis, T., Shen, J., Chen, D., Wen, F., Chen, Q., Guo, B.: RODIN: A generative model for sculpting 3d digital avatars using diffusion. In: IEEE/CVF Conference on Computer Vision and Pattern Recognition, CVPR 2023, Vancouver, BC, Canada, June 17–24, 2023. pp. 4563–4573. IEEE (2023). <https://doi.org/10.1109/CVPR52729.2023.00443>, <https://doi.org/10.1109/CVPR52729.2023.00443>
98. Wang, X., Wang, Y., Ye, J., Wang, Z., Sun, F., Liu, P., Wang, L., Sun, K., Wang, X., He, B.: Animatabledreamer: Text-guided non-rigid 3d model generation and reconstruction with canonical score distillation (2023)
99. Wang, Z., Lu, C., Wang, Y., Bao, F., Li, C., Su, H., Zhu, J.: Prolificdreamer: High-fidelity and diverse text-to-3d generation with variational score distillation. arXiv preprint arXiv:2305.16213 (2023)
100. Watson, D., Chan, W., Martin-Brualla, R., Ho, J., Tagliasacchi, A., Norouzi, M.: Novel view synthesis with diffusion models. ArXiv [abs/2210.04628](https://api.semanticscholar.org/abs/2210.04628) (2022), <https://api.semanticscholar.org/CorpusID:252780361>
101. Weng, H., Yang, T., Wang, J., Li, Y., Zhang, T., Chen, C.L.P., Zhang, L.: Consistent123: Improve consistency for one image to 3d object synthesis (2023)

102. Wu, R., Mildenhall, B., Henzler, P., Park, K., Gao, R., Watson, D., Srinivasan, P.P., Verbin, D., Barron, J.T., Poole, B., Holynski, A.: Reconfusion: 3d reconstruction with diffusion priors. arXiv (2023)
103. Xu, D., Yuan, Y., Mardani, M., Liu, S., Song, J., Wang, Z., Vahdat, A.: Agg: Amortized generative 3d gaussians for single image to 3d. arXiv preprint arXiv:2401.04099 (2024)
104. Xu, Y., Tan, H., Luan, F., Bi, S., Wang, P., Li, J., Shi, Z., Sunkavalli, K., Wetzstein, G., Xu, Z., Zhang, K.: Dmv3d: Denoising multi-view diffusion using 3d large reconstruction model. ArXiv **abs/2311.09217** (2023), <https://api.semanticscholar.org/CorpusID:265213192>
105. Yariv, L., Puny, O., Neverova, N., Gafni, O., Lipman, Y.: Mosaic-sdf for 3d generative models. arXiv preprint arXiv: 2312.09222 (2023)
106. Yu, A., Ye, V., Tancik, M., Kanazawa, A.: pixelnerf: Neural radiance fields from one or few images. In: IEEE Conference on Computer Vision and Pattern Recognition, CVPR 2021, virtual, June 19-25, 2021. pp. 4578–4587. Computer Vision Foundation / IEEE (2021). <https://doi.org/10.1109/CVPR46437.2021.00455>, https://openaccess.thecvf.com/content/CVPR2021/html/Yu_pixelNeRF_Neural_Radiance_Fields_From_One_or_Few_Images_CVPR_2021_paper.html
107. Yu, X., Xu, M., Zhang, Y., Liu, H., Ye, C., Wu, Y., Yan, Z., Liang, T., Chen, G., Cui, S., Han, X.: Mvimngnet: A large-scale dataset of multi-view images. In: CVPR (2023)
108. Zeng, X., Chen, X., Qi, Z., Liu, W., Zhao, Z., Wang, Z., FU, B., Liu, Y., Yu, G.: Paint3d: Paint anything 3d with lighting-less texture diffusion models (2023)
109. Zeng, Y., Wei, G., Zheng, J., Zou, J., Wei, Y., Zhang, Y., Li, H.: Make pixels dance: High-dynamic video generation. arXiv:2311.10982 (2023)
110. Zhang, R., Isola, P., Efros, A.A., Shechtman, E., Wang, O.: The unreasonable effectiveness of deep features as a perceptual metric. In: 2018 IEEE Conference on Computer Vision and Pattern Recognition, CVPR 2018, Salt Lake City, UT, USA, June 18-22, 2018. pp. 586–595. Computer Vision Foundation / IEEE Computer Society (2018). <https://doi.org/10.1109/CVPR.2018.00068>, http://openaccess.thecvf.com/content_cvpr_2018/html/Zhang_The_Unreasonable_Effectiveness_CVPR_2018_paper.html
111. Zhou, T., Tucker, R., Flynn, J., Fyffe, G., Snavely, N.: Stereo magnification. ACM Transactions on Graphics (TOG) **37**, 1 – 12 (2018), <https://api.semanticscholar.org/CorpusID:219893035>
112. Zhou, Z., Tulsiani, S.: Sparsefusion: Distilling view-conditioned diffusion for 3d reconstruction. In: CVPR (2023)
113. Zhu, J.Y., Zhang, Z., Zhang, C., Wu, J., Torralba, A., Tenenbaum, J.B., Freeman, B.: Visual object networks: Image generation with disentangled 3d representations. In: Neural Information Processing Systems (2018), <https://api.semanticscholar.org/CorpusID:54008375>
114. Zhu, J., Zhuang, P.: Hifa: High-fidelity text-to-3d with advanced diffusion guidance. CoRR **abs/2305.18766** (2023). <https://doi.org/10.48550/arXiv.2305.18766>, <https://doi.org/10.48550/arXiv.2305.18766>
115. Zhu, Z., Fan, Z., Jiang, Y., Wang, Z.: Fsgs: Real-time few-shot view synthesis using gaussian splatting (2023)
116. Zhuang, J., Wang, C., Lin, L., Liu, L., Li, G.: Dreameditor: Text-driven 3d scene editing with neural fields. In: Kim, J., Lin, M.C., Bickel, B. (eds.) SIGGRAPH Asia 2023 Conference Papers, SA 2023, Sydney, NSW, Australia, December 12-15, 2023. pp. 26:1–26:10. ACM (2023). <https://doi.org/10.1145/3610548.3618190>, <https://doi.org/10.1145/3610548.3618190>

117. Zou, Z.X., Yu, Z., Guo, Y.C., Li, Y., Liang, D., Cao, Y.P., Zhang, S.H.: Triplane meets gaussian splatting: Fast and generalizable single-view 3d reconstruction with transformers. arXiv preprint arXiv:2312.09147 (2023)